

## Fine particles production in sand under triaxial compression

Sadok Feia<sup>✉</sup>, Xavier Clain, Jean Canou, Jean Sulem, Siavash Ghabezloo

Laboratoire Navier, CERMES, Ecole des Ponts ParisTech, Marne-la-Vallée, Université Paris-Est, France

Received 7 March 2016

Revised 5 September 2016

Accepted 23 December 2016

Published online: 24 December 2016

### Keywords

Triaxial test

Granular materials

Grain breakage

Fine particles

**Abstract:** An experimental study, carried out in laboratory using a triaxial apparatus, proposes to evaluate the influence of grain size, grain shape and confining stress in fine particles production in sand specimen subjected to triaxial loading. 16 triaxial tests were conducted on specimens of an initial density index of 0.90 using the pluviation technique, with three different sands and under initial confining pressure of 100, 400, 800 and 1200 kPa. The experimental results show that the fine particles production is considerably affected by confining stresses, even at low values (100 kPa), and also by grain geometry. The experimental results show also that the fine particles production increase with the strain level during the shearing test.

© 2016 The authors. Published by the Faculty of Sciences & Technology, University of Biskra. This is an open access article under the CC BY license.

### 1. Introduction

Most reservoirs of oil and gas have a layer of water called natural formation water in the oil layer. For maximum recovery of oil, an amount of additional water is usually injected into the reservoir, which can be associated with hydrocarbon production. In the case of gas production, water may be condensed water. Consequently, during oil production, a large amount of water (one to three barrels per barrel of oil) is produced (Farajzadeh 2004). Re-injection of the water in the reservoir after a number of treatments and filtration is one of the best ways to remove the water; this technique was called PWRI (Produced Water Re-injection). This has the great advantage of maintaining the pressure in the reservoir, which simulates the production of oil (Li and Wong 2008, Farajzadeh 2004, Al-Abduwani et al. 2003). The re-injection of the produced water in oil reservoirs during production leads to a change in stress state, which can create shear bands in the formation. These bands are sources of grain crushing and creation of fine particles (Nguyen 2012). Crawford et al. (2004) carried out triaxial tests with different loading paths on Ottawa sand; they showed that the grain breakage is very important when the stress path becomes deviatoric. The intensity of grain crushing depends of stress level, grain resistance, and shear path (Feda 2002). These phenomena can lead to the formation of damaged zone causing a significant decrease of the reservoir permeability around the injectors and the injectivity of these wells.

Some authors have studied the fine particles production in a specimen subjected to a high pressure triaxial loading or oedometer loading (Lee and Farhoomand 1967, Hardin and Asce 1985, Chuhan et al. 2002, Dadda et al. 2015). Most of these studies use size analysis before and after shearing to quantify the amount of fine particles produced. They showed that the creation of fine particles after the test changes the particle size distribution of the tested sand. From these changes of the grain size distribution and using the empirical correlations, existing in literature, relating grain size with permeability (Hazen's 1911) we can estimate the new permeability of the soil after test (Lade et al. 1996).

The evolution of the fine particles production according to the deformation level of the specimen and the effect of some parameters such as the size and shape of the grains on the production of fine particles is currently poorly known. In the present study, a triaxial test campaign has been carried out on different types of sand, under different confining stresses to explore their impact along with the confining stress on the fine particles production

### 2. Experimental setting and specimen preparation

#### 2.1 Experimental setup

In this study, a classical triaxial cell has been used. The cylindrical specimens have a diameter of 100 mm and a height of 200 mm. The specimen is constituted with sand at density index of 0.90

<sup>✉</sup>Corresponding author. E-mail address: Sadok.feia@enpc.fr

and enveloped in a latex membrane which ensures the water tightness. The membrane is sealed at both the top and the bottom of the specimen to two bases which close the specimen. The stiffness of the specimen is provided by the isotropic confining pressure it undergoes during the test.

The base of the triaxial cell is placed on a movable part of a press whereas its fixed upper part abuts the specimen. A force sensor with a capacity of 32 kN and a 0.1% accuracy is used to measure the forces generated during the shear and thus to study the mechanical response of the sample. A displacement sensor LVDT measures the vertical displacement of the base of the press and thus the strain of the sample. Measuring the specimen volume during the test is made possible by using a flow-meter comprising a sealed chamber inside which slides a membrane whose displacement is measured by a second sensor LVDT. The displacement of the latter is related to the inputs and outputs of pore water in the specimen during the tests that are themselves representative of the variation in the volume of the specimen.

## 2.2 Sand description

Three different sands, Fontainebleau sand (NE34) and two cuts of Hostun sand (HN34 and HN31) are studied in the experimental program. Fontainebleau sand has sub-rounded grains, while Hostun sand has sub-angular grains as can be seen in the SEM images of figure 1.

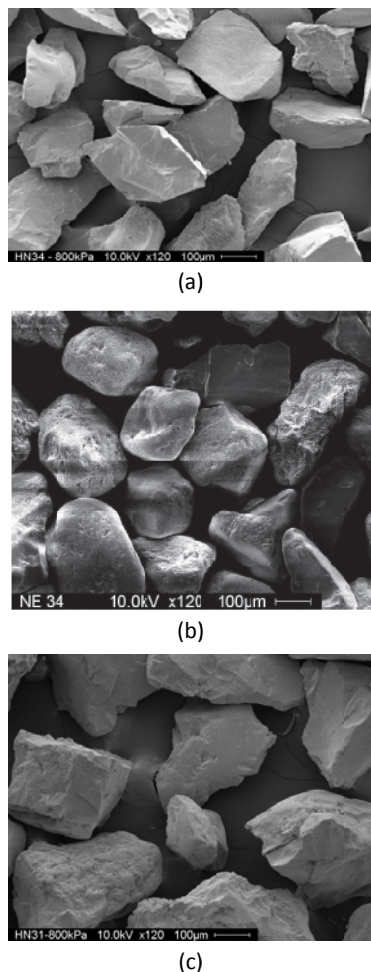


Fig. 1. SEM view of the sands studied: (a) HN34, (b) NE34, (c) HN31.

Table 1. Characteristics of sands used.

Sand	$d_{50}$ mm	$C_u$	Distribution	$e_{min}$	$e_{max}$	Angularity
NE34	0.21	1.5	uniform	0.557	0.884	Sub-rounded
HN31	0.32	1.3	uniform	0.674	1.014	Sub-angular
HN34	0.21	1.6	uniform	0.696	1.145	Sub-angular

All the sands consist mainly of silica grains (99%) and are commonly used in reference laboratory tests. Three different cuts are studied to explore the effects of different parameters. The characteristics of the tested materials are presented in Table 1 and the corresponding grain size distribution and pore access size curves are shown in figure 2. The pore access size distributions of the tested sands are evaluated by the tensiometric method (Feia et al. 2014).

Fontainebleau sand NE34 and sand Hostun HN34 have similar grain size distributions ( $d_{50} = 0.21$  mm) but differ in the shape of the grains. HN31 consists of Hostun sand with a  $d_{50}$  of 0.32 mm. Comparing the results obtained for the tests carried out on the three sands will permit to study the effects of following parameters on the pore size distribution:

- The effect of the mean grain size (HN31 vs HN34)
- The effect of the angularity of the grains (NE34 vs HN34)

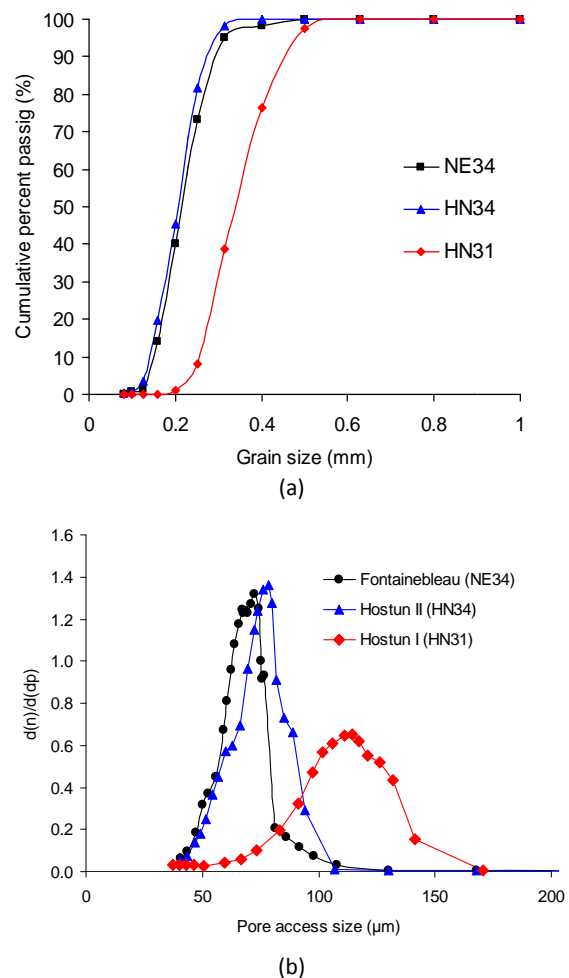


Fig. 2. (a) Grain size distribution (b) Pore access size distribution of the tested sands.

**2.3 Experimental procedure**

In order to validate the hypothesis that attrition and grain breaking can create fine particles during a triaxial compression test, we evaluate after the test the amount of fine particles within the specimen constituted of sand for which particles smaller than 80 μm have been removed by sieving prior to testing.

The first step is to carefully wash off the sand of its fine particles. The sand is first dried in a stove at 105°C for 48h and we then proceed by sieving it at 80 μm.

In this study the specimens have 200 mm height and 100 mm diameter and the setting up of the clipped sand is carried out by pluviation technique which can be considered as the closest natural deposition process (Benahmed et al., 2004).

In the pluviation technique, the sand is made on flow from a reservoir whose bottom consists of a grid of a certain opening (Figure 3). The desired density is achieved by controlling the height of pluviation (Vaid and Negusse, 1984) and the deposition intensity (Miura et Toki, 1982). The pluviation height is the vertical distance between the bottom surface of pluviation device and the surface of the sand previously filled by pluviation. To keep a constant height pluviation, it is necessary to constantly raise the pluviation device during construction of the specimen. The deposition intensity is the mass of sand falling on a unit of area per unit of time. It is controlled by the opening of the grid retaining the sand in the reservoir. For a same pluviation height, the density of the specimen increases when the deposition intensity decreases, which means when the opening of the grid decreases. (Kolbuszewski, 1948; Miura and Toki, 1982; Vaid and Negusse, 1984; Rad and Tumay, 1987; Levacher et al., 1994; Benahmed, 2001). It is also noted that with an equal open area, the outgoing flow of sand can vary as a function of the opening diameter of the grid holes; it is lower for small diameters.

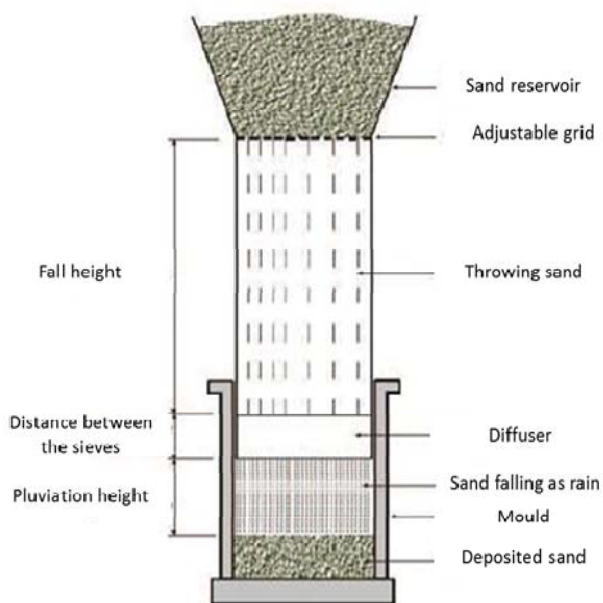


Fig. 3. Schematic diagram of pluviation process with diffuser (Benahmed, 2001).

To use the device for pluviation for specimen constitution at controlled density, it is first necessary to perform a calibration phase for determining the ascent rate of the engine and the density index obtained for each used configuration. We have for this calibration a mould whose interior dimensions are the same as those of the specimen to construct. Once the grid opening configuration chosen, the first step is to measure the speed of movement of sand front in the mould. This speed corresponds to the speed of the engine rise that we must adopt in order to keep a constant height pluviation.

For this study, the pluviation height is constant and fixed on 3cm. The second step is to fill the calibration mould in conditions of pluviation. This means that the base of the cylindrical body of the pluviator is placed in the center of the mould at 3cm from the bottom of the latter. The filling is started by opening the grid and by simultaneously moving the ascent motor. Once the mould is filled, the surface is levelled and then one weighs the contents sand.

The parameter which manages the state density of our specimen is the density index  $I_d$  and is defined by the relation (1):

$$I_D = \frac{e_{max} - e}{e_{max} - e_{min}} \tag{1}$$

Where  $e$  is the void ratio and  $e_{min}$  and  $e_{max}$  are respectively its minimum and maximum values for the considered sand obtained by ASTM D 4253.

In this calibration we have also used a mixture of Hostun sands (noticed Hn Mélange) in order to obtain a wider grain size distribution, keeping  $d_{50}$  equal to that of HN31. The obtained results for the four sands are shown in the graph of Figure 4 and represent the density index according to the deposition intensity. It appears first of all that it is possible, by this technique, to sweep a broad density index range (0.35 to 1) and one can access through this technique to density indices more difficult to obtain by conventional compaction methods.

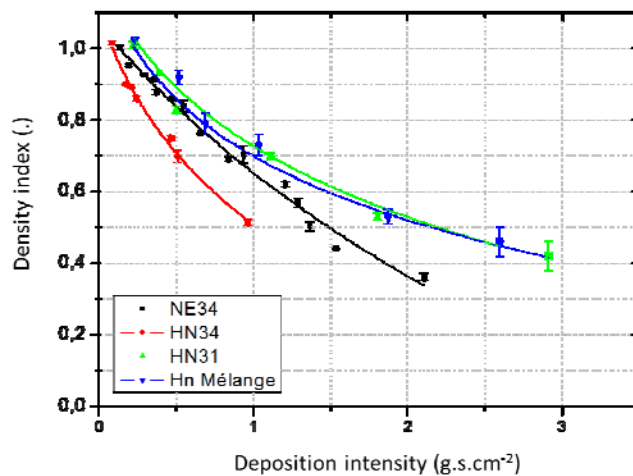


Fig. 4. Calibration curves of the density index obtained by pluviation for used sands.

We notice that at a constant deposition intensity, the density index of NE34 sand is higher than that of HN34 sand. These two sands have the same size and are distinguished by the angularity of their grains. We can then assume that the rounded grains of NE34 offer less resistance to the rearrangement of grains during the deposition phase and permit to obtain a higher density index.

In this study the specimen is sheared, as in a standard triaxial test, at a constant strain rate of 0.25%/min to a maximum axial strain of 18%. At the end of the test, the sheared sand specimen is collected and dried in a stove at 105°C for 48h before being sieved a second time at 80µm.

## 2.4 Experimental program

In the present study, tests were performed on Fontainebleau sand and two different cuts of Hostun sand under four confining stresses. The table 2 summarizes the characteristics of all tests performed.

## 3. Results and discussion

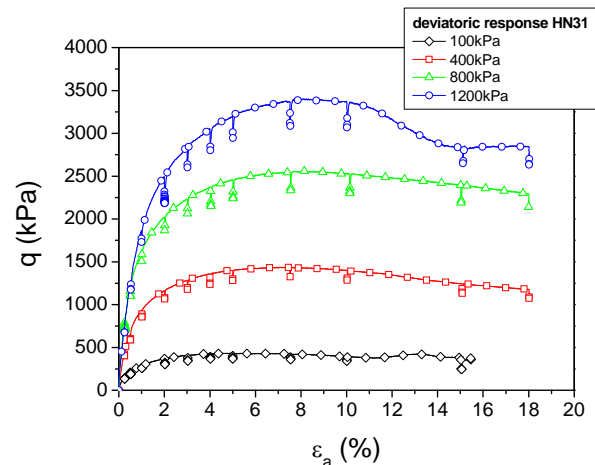
### 3.1 Mechanical behavior

Figure 5 shows a typical result of evolution of the stress deviator according to the axial strain for four values of confining pressure (100 to 1200 kPa) for HN31 sand. The specimens of sand have the same density index of 0.90 and are sheared to a maximum axial strain of 18%. We observe a classical type of response with quasi-linear stress evolution at low strains, followed by a nonlinear evolution up to maximum deviatoric. We observe then a softening phase during which the deviator decreases slowly. The curves end with a sharp fall in the deviator corresponding to a phase of strain localization.

In general, during shearing, the phase of locating and softening may be accompanied by the development of a well-defined shear plane inside the specimen in which the grains can slide over each other (Figure 6). The peak and ultimate friction angles are evaluated from these curves equal to  $\varphi_{max} = 37.3^\circ$  and  $\varphi_{ult} = 34^\circ$ . The evaluated values do not differ much for the other sand types, which can be attributed to the fact that the relative density and the mineralogy of the grains are the same for all specimens.

**Table 2.** Characteristics of tests.

Sand	$\sigma'_c$ (kPa)	Final axial strain (%)
NE34	100	18
NE34	400	18
NE34	800	18
NE34	1200	18
HN31	100	18
HN31	400	18
HN31	800	18
HN31	1200	18
HN34	100	18
HN34	400	18
HN34	800	18
HN34	1200	18
HN34	800	0
HN34	800	5.5
HN34	800	11
HN34	800	18



**Fig. 5.** Shear curves for four sands (HN31) under different confining pressures (100 kPa, 400 kPa, 800 kPa, 1200 kPa).

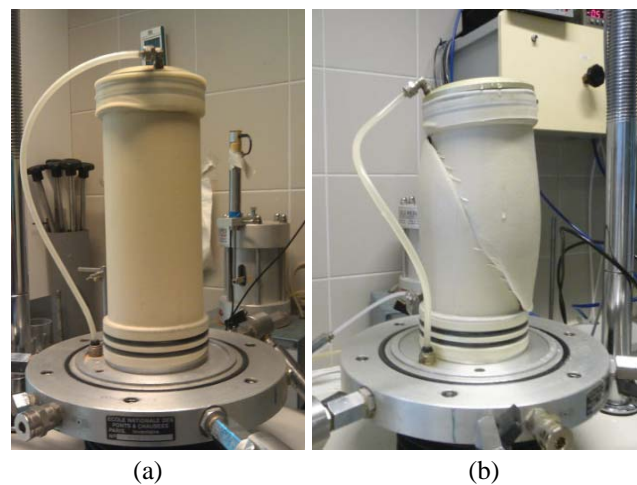


**Fig. 6.** Typical photographs of specimens (a) before test and (b) after test, under confining pressure of 100 kPa.

Figure 7 shows the evolution of the volumetric strain according to the axial strain. Volumetric strain curves have the same general appearance which can be divided into two phases: a first contracting phase where the volumetric strain decreases and a dilatant phase during which the specimen expands.

### 3.2 Comparison of the production of fine particles for different sands

Figure 8 presents a synthesis of the results in term of fine particles production for the three sands sheared under confining stresses from 100 kPa to 1200kPa. We observe that the mass of fine particles produced increases with the confining pressure. This result can be interpreted quite intuitively by the fact that the grains are pushed against each other by a superior stress as the confining stress increases, and consequently more subject to attrition and breaking. This increase is very low for Fontainebleau sand NE34 and much more significant for Hostun sands for which the fine particles production rate can be fifteen times higher than for Fontainebleau sand.

Hostun sand grains (HN34, HN31) present in the surface asperities which are fragile parts much more likely to break during shearing. On the contrary, Fontainebleau sand grains are

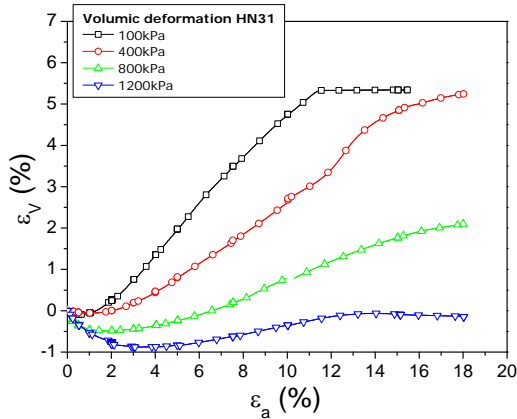


Fig. 7. Volumetric deformation curves for four sands (HN31) under different confining pressures (100 kPa, 400 kPa, 800 kPa, 1200 kPa).

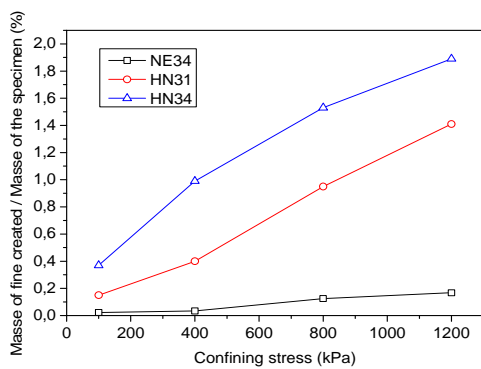


Fig. 8. Rate of fine particles created for different sands under four confining pressures.

sub-rounded and do not show any particular sensitivity. This has been verified on a view in a Scanning Electron Microscope (SEM) of fine particles created for Hostun sand and Fontainebleau sand (Figure 9). We can also observe that the HN31 sand ( $d_{50} = 320 \mu\text{m}$ ), coarser, presents a production of a smaller amount of fine particles than HN34 sand ( $d_{50} = 207 \mu\text{m}$ ). This can be attributed to the fact that the production of fine particles by attrition is related to the number of contact points between the grains of sand in the specimen.

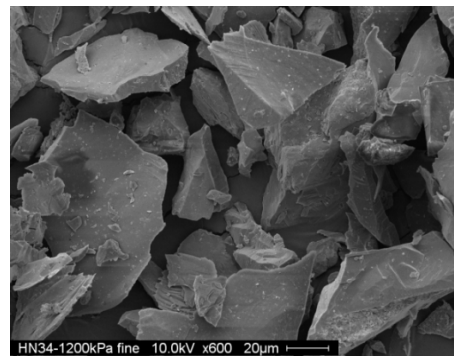
**3.3 Evolution of the fine particles production**

A series of triaxial tests was conducted to follow the evolution of the fine production during the shear phase. Four tests have been carried out on the HN34 sand consolidated under 800 kPa. The tests are interrupted at different steps corresponding to key values of axial strain (Figure 5):

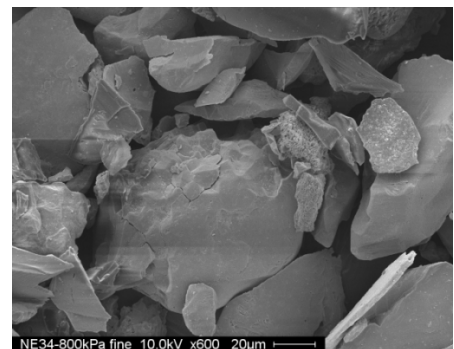
- 0%: just after the consolidation phase.
- 5,5% and 11% corresponding respectively to the half and the maximum values of deviatoric stress
- 18% corresponding to the maximum deformation reached

The Figure 10 presents the evolution of the fine particles production according to the axial strain. It is observed that the production of fine particles is evenly distributed during the test even if it is slightly accelerated from 5% of axial strain. We deduce that the phenomenon of attrition in the origin of this fine particles production is present from the beginning of shear and

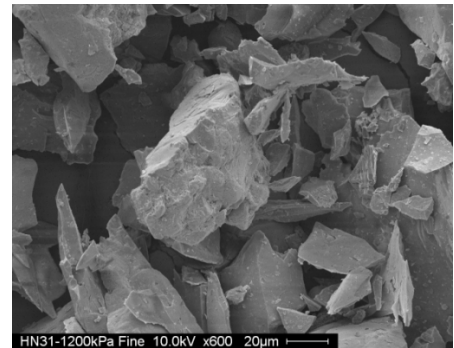
that is even more important when the shear band is imposed (from 5.5% of axial strain). It's interesting to note that these fine particles are the source of the decrease on the permeability in the sand specimen subjected to a triaxial test (Feia et al. 2016).



(a)



(b)



(c)

Fig. 9. SEM view of the fine particles created (a) HN34, (b) NE34, (c) HN31.

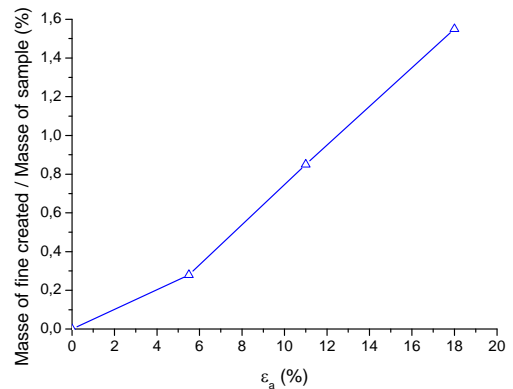


Fig. 10. Rate of fine particles created for different levels of axial strain under 800 kPa of confining stress.

#### 4. Conclusion

This article includes a presentation of the results of a study in laboratory about the fine particles production in sand specimens during a triaxial test. In this study, we tested three different sands, Fontainebleau sand (NE34) and two cats of Hostun sand (HN34, HN31), which allow to study the effect of grain shape (NE34 vs HN34) and grain size (HN34 vs HN31) on fine particles production. The tests were carried out on specimens with initial density index of 0.90 using pluviation technique, under four confining stresses 100, 400, 800, 1200 kPa. The results showed that the production of fine particles is not only influenced by the confining stress value, but by the grain geometry as well. Thus, it is showed that the asperities of angular grains and the number of contact points between grains both benefit the fine particles production. The measurement of the fine particles in different axial strain level showed that it is evenly distributed during the test.

#### References

- Al-Abduwani, F. A. H., A. Shirzadi, W. M. G. T. van den Broek, P. K. Currie (2005) Formation damage vs. solid particles deposition profile during laboratory-simulated PWRI. *Society of petroleum engineers journal* 10(2): 138–151.
- ASTM D 4253 (2006) Standard test methods for maximum index density and unit weight of soils using a vibratory table.
- Benahmed, N. (2001) Comportement mécanique d'un sable sous cisaillement monotone et cyclique: application aux phénomènes de liquéfaction et de mobilité cyclique. Thèse de doctorat, Ecole Nationale des Ponts et Chaussées, Marne-la-Vallée, France.
- Benahmed, N., J. Canou, J. C. Dupla (2004) Structure initiale et propriétés de liquéfaction statique d'un sable. *Comptes rendus mécanique* 332(11): 887-894.
- Chuhan, F.A., A. Kjeldstad, K. Bjørlykke, K. Høeg (2002) Porosity loss in Sand by Grain Crushing—Experimental Evidence and Relevance to Reservoir Quality. *Marine and Petroleum Geology* 19(1): 39-53.
- Crawford, B. R., M. J. Gooch, D. W. Webb (2004) Textural controls on constitutive behavior in unconsolidated sands: micromechanics and cap plasticity. *Proceedings of 6th Int. Conf. North American Rock Mechanics Symposium (NARMS)*. American Rock Mechanics Association, ARMA/NARMS 04-611
- Dadda, A., S. Feia, S. Ghabezloo, J. Sulem (2015) Fracturation des grains et l'évolution de la micro-structure d'un sable sous fortes contraintes. *Congrès Algérien de Mécanique (CAM 2015)*, El Oued 25-27 Octobre 2015.
- Farajzadeh, R. (2004) Produced water re-injection (pwri) an experimental investigation into internal filtration and external cake build up. Thesis, Faculty of Civil Engineering and Geosciences, Delft University of Technology.
- Feda, J. (2002) Notes on the effect of grain crushing on the granular soil behaviour. *Engineering Geology* 63(1-2): 93-98.
- Feia, S., J. Sulem, J. Canou, S. Ghabezloo, X. Clain (2016) Changes in permeability of sand during triaxial loading: effect of fine particles production. *Acta Geotechnica* 11(1): 1-19.
- Feia, S., S. Ghabezloo, J. F. Bruchon, J. Sulem, J. Canou, J. F. Dupla (2014) Experimental evaluation of the pore-access size distribution of sands. *Geotechnical Testing Journal* 37(4): 1-8.
- Hardin, B. O. (1985) Crushing of soil particles. *Journal of geotechnical Engineering* 111(10): 1177-1192.
- Hazen, A. (1911) Discussion of 'Dams on sand foundations' by A. C. Koenig. *Transactions of the American Society of Civil Engineers* 73: 199-203.
- Kolbuszewski, J. J. (1948) An experimental study of the maximum and minimum porosities of sands. 2nd International Conference Soil Mechanics Foundation Engineering, volume 1, Rotterdam.
- Lade, P. V. & J. A. Yamamuro (1996) Undrained sand behavior in axisymmetric tests at high pressures. *Journal of Geotechnical Engineering* 122(2): 120-129.
- Lee, K. L., I. Farhoomand (1967) Compressibility and crushing of granular soil in anisotropic triaxial compression. *Canadian Geotechnical Journal*, 4(1): 68-86.
- Levacher, D., J. Garnier, P. Chambon (1994) Reconstitution d'éprouvettes de sable: appareil de pluviation. *Revue française de la géotechnique* (68):49-56.
- Li, Z., R. C. K. Wong (2008) Estimation of suspended particle retention rate and permeability damage in sandstone from back analysis of laboratory injection tests. *Proceedings of canadian international petroleum conference*. Society of Petroleum Engineers.
- Miura, S., S. Toki (1982) A sample preparation method and its effect on static and cyclic deformation strength properties of sand. *Soils and Foundations* 22(1): 61-77.
- Nguyen, V.H. (2012) Compaction des roches réservoirs peu ou non consolidées: impacts sur les propriétés de transport. Thèse de doctorat, Université de Cergy-Pontoise.
- Rad, N.S., M.T. Tumay (1987) Factors affecting sand specimen preparation by raining. *ASTM Geotechnical Testing Journal* 10(1): 31-57.
- Vaid, Y.P., D. Negussey (1984) Relative density of air and water pluviated sand. *Soils and Foundations* 4(2): 101-105.